Defect Properties the Two-Dimensional (CH₃NH₃)₂Pb(SCN)₂I₂ Perovskite: A Density Functional Theory Study

Zewen Xiao,[a] Weiwei Meng,[a,b] Jianbo Wang,[b] and Yanfa Yan*[a]

Abstract: Recently, solar cells based on 2D (CH₃NH₃)₂Pb(SCN)₂I₂ perovskite have realized a power conversion efficiency of 3.23%. In this work, we study the defect properties of (CH₃NH₃)₂Pb(SCN)₂I₂ through density-functional theory calculations. It is found that the lower crystal structure dimensionality of MA2Pb(SCN)2I2 makes the valence band maximum lower and the conduction band minimum higher as compared to its 3D CH₃NH₃PbI₃ perovskite counterpart, resulting in relatively deeper defect transition levels. Our calculated defect formation energies suggest that if the (CH₃NH₃)₂Pb(SCN)₂I₂ perovskite absorbers are synthesized under Pb-poor and I-rich conditions, the dominant defects should be Pb vacancies, which create shallow levels. The resultant perovskite films are expected to exhibit p-type conductivity with a relatively long carrier lifetime.

Solar cells based on polycrystalline organic-inorganic lead halide perovskite films have realized a remarkable improvement in the power conversion efficiency (PCE) over the last six years. showing a current record PCE of over 22%. [1,2] However, some significant challenges must be resolved before this photovoltaic technology can be commercialized. One of the challenges is that lead halide perovskite absorbers react with moisture quickly and degrade to PbI₂, losing the excellent photovoltaic properties. [3,4] So far, extensive efforts have primarily focused on mitigating the moisture-induced degradation of perovskite solar cells. Besides encapsulating the devices using glass plates or moisture resistive polymers such as nanotube embedded polymer matrix (PMMA),[5,6] adding hydrophobic cations into the perovskite absorbers has also been used to improve the moisture resistivity. [7-9] On the anion site, it has been reported that adding pseudohalide SCN- can improve the moisture resistance of the perovskite absorbers.[10,11] Recent reports have shown that after adding pseudohalide SCN-, the absorber becomes a 2D perovskite with a composition of (MA)₂Pb(SCN)₂I₂ (MA: CH₃NH₃) (see the crystal structure in Figure 1a).[12,13] It was further found that this 2D perovskite has a bandgap of slightly over 2.0 eV with a large absorption coefficient. [14,15] The carriers are mobile, but are confined in the 2D layers. [14,16] It was also suggested that this 2D perovskite could be considered for use as an absorber for the top cell of a tandem solar cell, if films could be grown with the 2D layers aligned perpendicular to the substrate. [14]

More recently, solar cells based on $(MA)_2Pb(SCN)_2l_2$ absorbers have realized a PCE of $3.23\%.^{[12]}$ Considering the large bandgap and the layered structure, this PCE value is

perovskite-based solar cells.^[17,18] Furthermore, the reported (MA)₂Pb(SCN)₂l₂ films were highly orientated along the (100) direction,^[12,14] which is unfavorable for solar cell device application due to the strong anisotropic transport and optical properties of (MA)₂Pb(SCN)₂l₂. As we previously pointed out, if the (MA)₂Pb(SCN)₂l₂ films were grown with the 2D layers perpendicular to the substrate, similar to the 1D Sb₂Se₃ photovoltaics reported by Zhou *et al.*,^[19] the transport and optical properties, and, therefore, the PCE could be significantly improved. To understand fully the potential of the 2D (MA)₂Pb(SCN)₂l₂ perovskite for solar cell applications, it is important to study the defect properties of this 2D absorber, as the results may provide valuable guidance for further improving the performance of (MA)₂Pb(SCN)₂l₂-based solar cells and also have implication for other prospective optoelectronic application.

surprisingly high and better than other 2D single-layered

In this work, we present a density functional study on the defect properties of 2D $(MA)_2Pb(SCN)_2l_2$ perovskite. We find that this layered material may exhibit defect properties suitable for solar cell applications, if the absorbers are synthesized using Pb-poor/I-rich conditions. In this case, the dominant defects should be Pb vacancies, which create shallow levels. The absorber layers are then expected to have long carrier lifetime and exhibit a p-type conductivity.

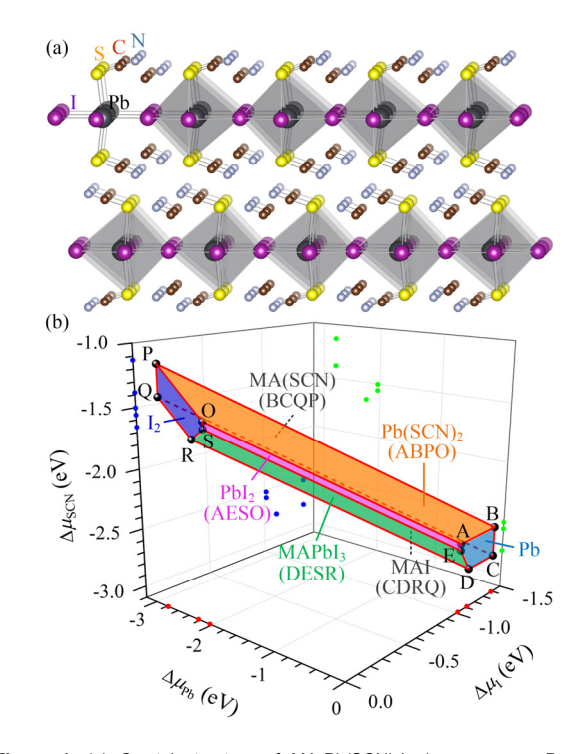


Figure 1. (a) Crystal structure of $MA_2Pb(SCN)_2l_2$ (space group $Pnm2_1$). Hydrogen atoms are not shown for clarity. (b) Calculated polyhedron of the chemical potential region in which $MA_2Pb(SCN)_2l_2$ is stable against possible competing phases, including Pb, l_2 , MAI, Pbl_2 , MA(SCN), $Pb(SCN)_2$, and $MAPbl_3$.

 [[]a] Dr. Z. Xiao, W. Meng, Prof. Dr. Y. Yan
 Department of Physics and Astronomy, and Wright Center for
 Photovoltaic Innovation and Commercialization
 The University of Toledo
 Toledo. Ohio 43606 (USA)

E-mail: yanfa.yan@utoledo.edu b] W. Meng, Prof. Dr. J. Wang

W. Meng, Prof. Dr. J. Wang School of Physics and Technology, Center for Electron Microscopy, MOE Key Laboratory of Artificial Micro- and Nano-structures, and Institute for Advanced Studies
 Wuhan 430072 (China)

Figure 1b shows the calculated chemical potential window, in which, $MA_2Pb(SCN)_2l_2$ is stabilized against possible competitive phases including Pb, l_2 , MAI, MA(SCN), Pbl $_2$ and Pb(SCN) $_2$. The chemical potential window polyhedron has a long but narrow shape, as is typical for halide perovskites, $l_2^{20,21}$ indicating that the chemical growth condition should be carefully controlled to form pure $MA_2Pb(SCN)_2l_2$ phase.

The photovoltaic properties of an absorber are partially determined by the defect properties of the absorber including the charge-state transition levels and formation energies of point defects. We first calculated the charge-state transition levels for intrinsic acceptor-like (red) and donor-like (blue) defects in MA₂Pb(SCN)₂I₂, as shown in Figures 2a and 2b, respectively. V_{MA} is a shallow acceptor with the (0/1-) transition level at 0.06 eV above the valence band maximum (VBM), which is primarily due to the highly ionic nature of the MA+ anion. VPb exhibits a shallow (0/1-) transition level right at the VBM, but a deep (1-/2-) transition level at 0.44 eV above the VBM. V_I has a deep (0/1+) transition level at 0.40 eV below the conduction band minimum (CBM). Compared with V_{I} , V_{SCN} shows a shallower (0/1+) transition level at 0.11 eV below the CBM, which should be attributed to the stronger ionicity for the SCN- anion than for the I- anion. MA_i has a shallow (0/1+) transition level at 0.14 eV below the CBM, again, because of the high ionicity of the MA+ cation. In contrast, the Pbi has a very deep (0/2+) transition level at 0.86 eV below the CBM, because of the lower ionicity of Pb. Both I_i and SCN_i have shallow (0/1-) transition levels (0.10 eV and 0.06 eV, respectively, above the VBM. The slightly shallower (0/1-) transition level of SCN_i than that of I_i, again, could be attributed to the higher ionicity of the SCN- anion than the I- anion. The behavior of an antisite can be qualitatively understood as a pair of interstitial and vacancy. MAPb antisite, which can be viewed as a combination of MAi and VPb, has a relatively shallow (0/1-) transition at 0.15 eV above the VBM, which is understood from the shallow nature of both MA_i and V_{Pb}. Pb_{MA} antisite (viewed as Pb_i + V_{MA}) also has a relatively shallow (0/1+) transition at 0.11 eV below the CBM, despite the deep nature of Pbi which features the formation of a covalent Pb dimer. All the other antisites have deep transition levels in the bandgap, as seen in Figure 2.

Compared with those in 3D MAPbl₃,^[20,22] the defect transition levels in 2D MA₂Pb(SCN)₂I₂ are generally deeper. This can be understood based on the differences of the electronic structures and the band edge positions of these perovskites. Figure 3 shows the alignments of the experimental band edge positions (referred to the vacuum level) of the 3D MAPbl₃ and 2D MA₂Pb(SCN)₂I₂ perovskites, with the transition levels of the dominant defects, V_{Pb} and V_I, being shown. The VBM positions for MAPbI₃ and MA₂Pb(SCN)₂I₂ were reported to be -5.4 eV^[23] and -5.7 eV,[12] respectively. Considering the bandgaps of 1.5 eV[23] and 2.3 eV,[15] the CBM positions of MAPbI₃ and MA₂Pb(SCN)₂I₂ are calculated to be at -3.9 eV and -3.4 eV, respectively. As we reported previously, because of the electronic confinement along the interlayer direction, the VBM and CBM of 2D MA₂Pb(SCN)₂I₂ become less dispersive, leading to the lower VBM and the higher CBM, as compared with 3D MAPbl₃. As seen in Figure 3, the (0/1-) and (1-/2-) transition levels of V_{Pb} and the (0/1+) transition level of V_{I} (and also V_{SCN}) in 2D MA₂Pb(SCN)₂I₂ and 3D MAPbI₃, to some degree, are similar with respect to the vacuum level. Therefore, the lower VBM and the higher CBM make the transition levels of acceptors such as V_{Pb} and donors such as V_{I} deeper with respect to the band edge positions.

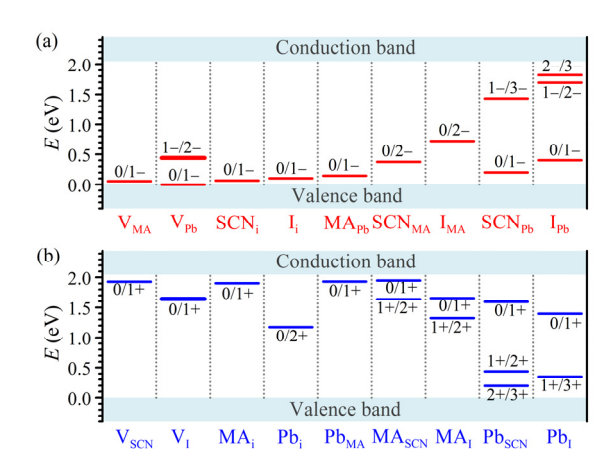


Figure 2. Calculated charge-state transition energy levels for intrinsic (a) acceptors and (b) donors in MA₂Pb(SCN)₂I₆.

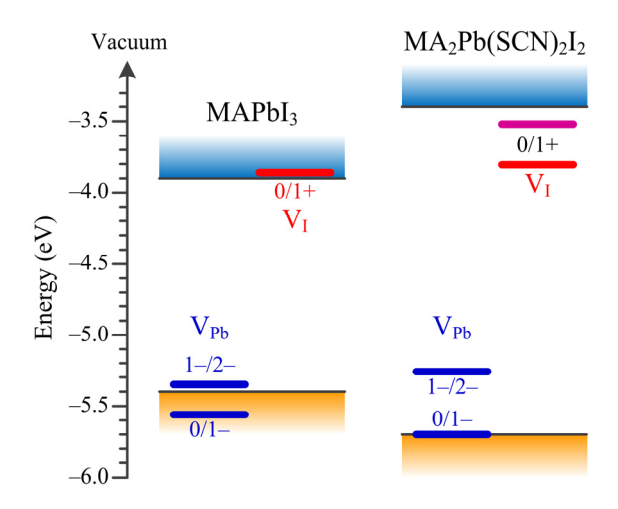


Figure 3. Alignment of VBM and CBM positions and defect transition levels with respect to the vacuum level of 3D MAPbl $_3$ and 2D MA $_2$ Pb(SCN) $_2$ I $_2$ perovskites. The experimental VBM positions of $-5.4~eV^{[23]}$ and $-5.7~eV^{[12]}$ and bandgaps of 1.5 eV and 2.3 eV $^{[15]}$ are used for MAPbI $_3$ and MA $_2$ Pb(SCN) $_2$ I $_2$, respectively. The defect transition levels of MAPbI $_3$ are taken from Ref. $^{[20]}$.

We have further calculated the formation energies of the above point defects. Here, we chose two representative chemical potential points in Figure 1b for the following discussion; P ($\Delta\mu_{Pb}=-2.78$ eV, $\Delta\mu_{I}=0$ eV, $\Delta\mu_{SCN}=-1.13$ eV and $\Delta\mu_{MA}=-3.97$ eV; denoted as "Pb-poor/I-rich") and B ($\Delta\mu_{Pb}$

= 0 eV, $\Delta\mu_{\rm I}$ = - 1.39 eV, $\Delta\mu_{\rm SCN}$ = - 2.52 eV and $\Delta\mu_{\rm MA}$ = - 2.58 eV, denoted as "Pb-rich/I-poor"). The calculated formation energies

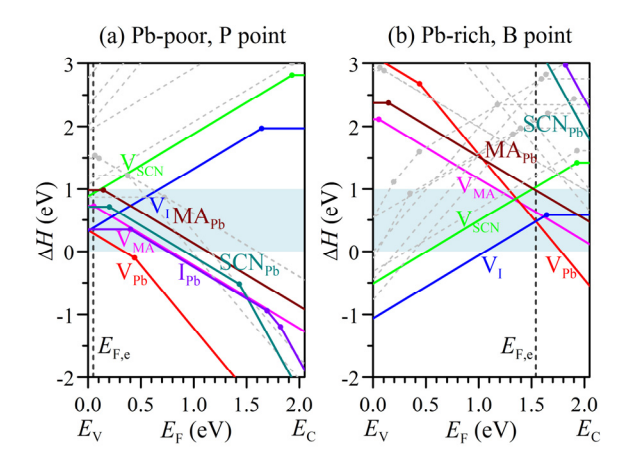


Figure 4. Calculated formation enthalpies ΔH of intrinsic defects in MA₂Pb(SCN)₂l₂ as a function of Fermi level $E_{\rm F}$ at two representative chemical potential points in Figure 2, (a) P (Pb-poor) and (b) B (Pb-rich). Defects with very high ΔH values are shown by dashed lines. The vertical dashed lines mark the calculated equilibrium Fermi level $E_{\rm Fe}$ at T=300 K.

 ΔH of the intrinsic defects as a function of E_F at these chemical points are plotted in Figures 4a and 4b. Under the Pb-poor condition, V_{Pb} has the lowest ΔH over essentially the whole E_{F} region and is the dominant defect, which should be mainly responsible for the intrinsic p-type conductivity of $MA_2Pb(SCN)_2I_2$ films reported by Liu *et al.*^[12] I_{Pb} also has low ΔH , but is stabilized in the neutral charge state in the highly p-type region (E_F < 0.40 eV), and therefore has little contribution to the p-type conductivity. For quantitative analysis, the equilibrium $E_{\rm F}$ $(E_{\rm F,e})$ at 300 K (i.e., growth and defect formation at room temperature) was calculated by considering all the ΔH values and the semiconductor statistics, [24,25] giving $E_{F,e} - E_V = 0.05 \text{ eV}$ and a hole concentration as high as 5.2×10¹⁸ cm⁻³. As the (1–/2–) transition level of V_{Pb} and the (0/1–) transition level of I_{Pb} are \sim 0.4 eV above the $E_{\rm F,e}$, there is little possibility for these transitions to occur, which, therefore, won't be recombination centers. As the chemical potential point shifts from the Pb-poor side to Pb-rich side, the ΔH of the acceptor defects including V_{Pb} and V_{MA} increase, while those of the donor defects including V_{I} and V_{SCN} decrease. Under the Pb-rich condition, the ΔH dominant donor V_I and the dominant acceptor V_{Pb} intersect at a n-type $E_{\rm F}$ of 1.54 eV above the VBM (i.e., 0.50 eV below the CBM), where the E_F is pinned by the formation of compensating V_{Pb}²⁺ and V_I⁻ charged defects, indicating a compensated *n*-type conductivity. For quantitative analysis, the electron concentration at $E_C - E_V = 0.50$ eV was estimated to be 1.1×10^{11} cm⁻³ at 300 K. As the dominant defect V_I has a (0/1+) transition level just above the $E_{F,e}$, it is likely to behave as a recombination center, which should be avoided for photovoltaic applications. These theoretical results indicate that the electrical properties of MA₂Pb(SCN)₂I₂ can range from high-density p-type to lowdensity *n*-type, depending on the growth condition. It is suggested that the MA₂Pb(SCN)₂I₂ films should be synthesized under the Pb-poor condition in order to realize good *p*-type conduction and maximize the photovoltaic performance. It should be pointed out that the *p*-type MA₂Pb(SCN)₂I₂-based solar cells have initially a PCE of 3.23%, which is not a bad start for a 2D absorber material. The PCE may be improved if further material and device optimizations are performed.

In summary, we have investigated the defect properties of 2D MA $_2$ Pb(SCN) $_2$ I $_2$ perovskite by DFT study. It is found that the lower crystal structure dimensionality of MA $_2$ Pb(SCN) $_2$ I $_2$ makes the VBM lower and the CBM higher as compared to its 3D MAPbI $_3$ perovskite counterpart, resulting in relatively deeper defect transition levels. Our calculated defect formation energies suggest that for optimal photovoltaic applications, the 2D MA $_2$ Pb(SCN) $_2$ I $_2$ perovskite absorber layers should be synthesized under Pb-poor and I-rich conditions so that the dominant defects are V_{Pb}, which create shallow defect transition levels. The thin films synthesized under these conditions should be intrinsically p-type.

Experimental Section

Total-energy defect calculations were performed with the VASP code, [26] using a plane wave cutoff energy of 400 eV and the Γonly k-mesh for the 400-atoms supercell ($2\sqrt{2}\times2\sqrt{2}\times1$ unit cells). The generalized gradient approximation (GGA) Perdew-Burke-Ernzerhof (PBE)[27] was used for exchange-correlation functional. Our previous work has shown that the PBE functional predicts reasonable well the bandgap of for MA₂Pb(SCN)₂I₂[14] primarily because the underestimation due to the well-known standard DFT bandgap error and the overestimation due to the exclusion of spin-orbit coupling (SOC) cancel each other.[28] Moreover, previous reports have shown that the PBE non-SOC method gives reasonably good predictions for the electronic, optical and defect properties for lead halide perovskites. [20,22,29] The atomic positions of the defect structures were relaxed until the total force on each atom was smaller than 0.05 eV/Å. The potential-alignment, image charge and bond-filling corrections were applied by the methodology described in the literatures.[21,30] For a defect (D) in a charge state q, the formation enthalpy is calculated through the equation[31]

 $\Delta H_{D,q} \ (\mu, E_F) = (E_{D,q} - E_H) - \Sigma n_\alpha \mu_\alpha + q(E_F + E_V),$ (1) where $(E_{D,q} - E_H)$ is the energy difference between the defect and host supercells. n_α indicates the number of α atoms added $(n_\alpha > 0)$ or removed $(n_\alpha < 0)$ when a defect is formed, and μ_α is the chemical potential of the α atom, which can be expressed with respect to that of the elemental phase $(\mu_\alpha^{\rm el})$ by $\mu_\alpha = \mu_\alpha^{\rm el} + \Delta \mu_\alpha$. E_F is the Fermi level referred to the VBM, E_V . The μ_α value varies depending on the experimental conditions. The equilibrium Fermi levels $(E_{F,e})$ were determined using the calculated density of states (DOS) by solving semiconductor statistic equations self-consistently so as to satisfy the charge neutrality condition. $[^{24,33}]$

The chemical potential window of the 2D $MA_2Pb(SCN)_2I_2$ is determined using three steps. First, to stabilize the $MA_2Pb(SCN)_2I_2$ phase, the following thermodynamic equilibrium must be reached:

$$2\Delta\mu_{MA} + \Delta\mu_{Pb} + 2\Delta\mu_{SCN} + 2\Delta\mu_{I} = \Delta H (MA_2Pb(SCN)_2I_2) =$$

-12.98eV, (2)

where ΔH (MA₂Pb(SCN)₂I₂) is the formation enthalpy of MA₂Pb(SCN)₂I₂, as referred to the elemental solids Pb (cubic structure, space group Fm–3m) and I₂ (orthorhombic, Cmca), and organic groups CH₃NH₃ (MA) and SCN (i.e., assuming gas models). Second, to exclude the elemental phases, it is required that $\Delta \mu_{\rm MA} < 0$, $\Delta \mu_{\rm Pb} < 0$, $\Delta \mu_{\rm SCN} < 0$, and $\Delta \mu_{\rm I} < 0$. Third, to avoid the formation of the competing secondary phases including MAI (tetragonal, space group P4/nmm), [34] PbI₂ (trigonal, P–3m1), [35] MA(SCN) (following Cs(SCN), orthorhombic, Pnma), [36] Pb(SCN)₂ (monoclinic, C2/c), [37] and MAPbI₃ (tetragonal, I4/mcm), [38] the following equations also must be satisfied:

$$\Delta\mu_{MA} + \Delta\mu_{I} < \Delta H \text{ (MAI)} = -3.72 \text{ eV}$$
 (3)
 $\Delta\mu_{MA} + \Delta\mu_{SCN} < \Delta H \text{ (MA(SCN))} = -5.10 \text{ eV}$ (4)
 $\Delta\mu_{Pb} + 2\Delta\mu_{I} < \Delta H \text{ (PbI}_{2}) = -2.04 \text{ eV}$ (5)
 $\Delta\mu_{Pb} + 2\Delta\mu_{SCN} < \Delta H \text{ (Pb(SCN)}_{2}) = -5.04 \text{ eV}$ (6)
 $\Delta\mu_{MA} + \Delta\mu_{Pb} + 3\Delta\mu_{I} < \Delta H \text{ (MAPbI}_{3}) = -5.95 \text{ eV}$ (7)

Under the above constraints, the allowed $\Delta\mu_{Pb}$, $\Delta\mu_{I}$, and $\Delta\mu_{SCN}$ for single-phase MA₂Pb(SCN)₂I₂ are bound in a polyhedron as shown in Figure 1b, whereas $\Delta\mu_{MA}$ is associated with $\Delta\mu_{Pb}$, $\Delta\mu_{I}$, and $\Delta\mu_{SCN}$ through equation (2).

Keywords: intrinsic defects • two-dimensional • perovskite • thiocyanates

Acknowledgements

This work was funded in part by the Office of Energy Efficiency and Renewable Energy (EERE), U.S. Department of Energy, under Award Number DE-EE0006712, and the Ohio Research Scholar Program. This research used the resources of the Ohio Supercomputer Center and the National Energy Research Scientific Computing Center, which is supported by the Office of Science of the U.S. Department of Energy under Contract No. DE-AC02-05CH11231.

- [1] A. Kojima, K. Teshima, Y. Shirai, T. Miyasaka, J. Am. Chem. Soc. 2009, 131, 6050–6051.
- [2] National Renewable Energy Laboratory (NREL), "Best Research-Cell Efficiencies," can be found under http://www.nrel.gov/ncpv/images/efficiency_chart.jpg, n.d.
- [3] J. M. Frost, K. T. Butler, F. Brivio, C. H. Hendon, M. van Schilfgaarde, A. Walsh, Nano Lett. 2014, 14, 2584–2590.
- [4] G. Niu, W. Li, F. Meng, L. Wang, H. Dong, Y. Qiu, J. Mater. Chem. A 2014, 2, 705–710.
- [5] Y. Han, S. Meyer, Y. Dkhissi, K. Weber, J. M. Pringle, U. Bach, L. Spiccia, Y.-B. Cheng, J. Mater. Chem. A 2015, 3, 8139–8147.
- [6] S. N. Habisreutinger, T. Leijtens, G. E. Eperon, S. D. Stranks, R. J. Nicholas, H. J. Snaith, *Nano Lett.* 2014, 14, 5561–5568.
- [7] I. C. Smith, E. T. Hoke, D. Solis-Ibarra, M. D. McGehee, H. I. Karunadasa, Angew. Chemie 2014, 126, 11414–11417.

- [8] S. Yang, Y. Wang, P. Liu, Y.-B. Cheng, H. J. Zhao, H. G. Yang, Nat. Energy 2016, 15016.
- [9] A. Mei, X. Li, L. Liu, Z. Ku, T. Liu, Y. Rong, M. Xu, M. Hu, J. Chen, Y. Yang, et al., Sci. 2014, 345, 295–298.
- [10] Q. Jiang, D. Rebollar, J. Gong, E. L. Piacentino, C. Zheng, T. Xu, Angew. Chemie 2015, 127, 7727–7730.
- [11] Y. Chen, B. Li, W. Huang, D. Gao, Z. Liang, Chem. Commun. 2015, 51, 11997–11999.
- [12] J. Liu, J. Shi, D. Li, F. Zhang, X. Li, Y. Xiao, S. Wang, Synth. Met. 2016, 215, 56–63.
- [13] M. Daub, H. Hillebrecht, Angew. Chemie Int. Ed. 2015, 54, 11016– 11017.
- [14] Z. Xiao, W. Meng, B. Saparov, H.-S. Duan, C. Wang, C. Feng, W.-Q. Liao, W. Ke, D. Zhao, J. Wang, et al., J. Phys. Chem. Lett. 2016, 7, 1213–1218.
- [15] D. Umeyama, Y. Lin, H. I. Karunadasa, Chem. Mater. 2016, 28, 3241–3244.
- [16] M. E. Kamminga, H.-H. Fang, M. R. Filip, F. Giustino, J. Baas, G. R. Blake, M. A. Loi, T. T. M. Palstra, *Chem. Mater.* 2016, acs.chemmater.6b00809.
- [17] M. Lyu, J.-H. Yun, M. Cai, Y. Jiao, P. V. Bernhardt, M. Zhang, Q. Wang, A. Du, H. Wang, G. Liu, et al., Nano Res. 2016, 9, 1–11.
- [18] B.-W. Park, B. Philippe, X. Zhang, H. Rensmo, G. Boschloo, E. M. J. Johansson, *Adv. Mater.* 2015, 27, 6806–6813.
- [19] Y. Zhou, L. Wang, S. Chen, S. Qin, X. Liu, J. Chen, D.-J. Xue, M. Luo, Y. Cao, Y. Cheng, et al., Nat. Photonics 2015, 9, 409–415.
- [20] W.-J. Yin, T. Shi, Y. Yan, Appl. Phys. Lett. 2014, 104, 063903.
- [21] Z. Xiao, Y. Zhou, H. Hosono, T. Kamiya, Phys. Chem. Chem. Phys. 2015, 17, 18900–18903.
- [22] M. L. Agiorgousis, Y. Sun, H. Zeng, S. Zhang, J. Am. Chem. Soc. 2014, 136, 14570–14575.
- [23] P. Schulz, E. Edri, S. Kirmayer, G. Hodes, D. Cahen, A. Kahn, Energy Environ. Sci. 2014, 7, 1377.
- [24] Z. Xiao, F.-Y. Ran, H. Hosono, T. Kamiya, Appl. Phys. Lett. 2015, 106, 152103.
- [25] F.-Y. Ran, Z. Xiao, Y. Toda, H. Hiramatsu, H. Hosono, T. Kamiya, Sci. Rep. 2015, 5, 10428.
- [26] G. Kresse, J. Furthmüller, *Phys. Rev. B* **1996**, *54*, 11169–11186.
- [27] J. P. Perdew, K. Burke, M. Ernzerhof, Phys. Rev. Lett. 1996, 77, 3865–3868.
- [28] E. Mosconi, A. Amat, M. K. Nazeeruddin, M. Grätzel, F. De Angelis, J. Phys. Chem. C 2013, 117, 13902–13913.
- [29] M.-H. Du, J. Phys. Chem. Lett. 2015, 6, 1461–1466.
- [30] S. Lany, A. Zunger, *Phys. Rev. B* **2008**, *78*, 235104.
- [31] C. G. Van de Walle, J. Neugebauer, J. Appl. Phys. 2004, 95, 3851–3879.
- [32] Y. Yan, S. H. Wei, Phys. Status Solidi B 2008, 245, 641-652.
- [33] D. B. Laks, C. G. Van de Walle, G. F. Neumark, P. E. Blöchl, S. T. Pantelides, *Phys. Rev. B* 1992, 45, 10965–10978.
- [34] H. Ishida, H. Maeda, A. Hirano, T. Fujimoto, Y. Kubozono, S. Kashino, S. Emura, Zeitschrift für Naturforsch. A 1995, 50, 876–880.
- [35] B. Palosz, J. Phys. Condens. Matter 1990, 2, 5285–5295.
- [36] S. Manolatos, M. Tillinger, B. Post, J. Solid State Chem. 1973, 7, 31–35.
- [37] J. A. A. Mokuolu, J. C. Speakman, Acta Crystallogr. Sect. B Struct.

Crystallogr. Cryst. Chem. 1975, 31, 172–176.

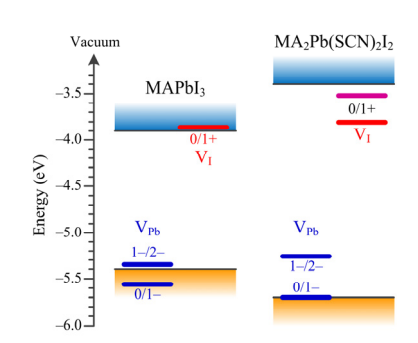
Hansen, Chem. Commun. 2015, 51, 4180-4183.

[38] M. T. Weller, O. J. Weber, P. F. Henry, A. M. Di Pumpo, T. C.

Entry for the Table of Contents

COMMUNICATION

To optimize the photovoltaic performance, the 2D MA $_2$ Pb(SCN) $_2$ I $_2$ perovskite absorber layers should be synthesized under Pb-poor and I-rich conditions so that the dominant defects are V $_{\text{Pb}}$, which create shallow defect transition levels and making the absorber layers intrinsically p-type.



Z. Xiao, B. Saparov, W. Meng, H.-S. Duan, J. Wang, D.B. Mitzi,* and Y. Yan*

Page No. – Page No.

Defect properties.